W
LBL-18441
UC66a c.1

Lawrence Berkeley Laboratory

UNIVERSITY OF CALIFORNIA

RECEIVED
LAWRENCE
BERKELEY LABORATORY
MAR 26 1985
LIBRARY AND
DOCUMENTS SECTION

EARTH SCIENCES DIVISION

Presented at the 10th Annual Workshop on Geothermal Reservoir Engineering, Stanford University, Stanford, CA, January 22-24, 1985; and to be published in the Proceedings

For Reference
Not to be taken from this room

A NEW MODEL FOR WELL TEST ANALYSIS IN A PURELY FRACTURED MEDIUM

K. Karasaki, J.C.S Long, and P.A. Witherspoon

January 1985

LBL-18441
c.1

Prepared for the U.S. Department of Energy under Contract DE-AC03-76SF00098

DISCLAIMER

This document was prepared as an account of work sponsored by the United States Government. While this document is believed to contain correct information, neither the United States Government nor any agency thereof, nor the Regents of the University of California, nor any of their employees, makes any warranty, express or implied, or assumes any legal responsibility for the accuracy, completeness, or usefulness of any information, apparatus, product, or process disclosed, or represents that its use would not infringe privately owned rights. Reference herein to any specific commercial product, process, or service by its trade name, trademark, manufacturer, or otherwise, does not necessarily constitute or imply its endorsement, recommendation, or favoring by the United States Government or any agency thereof, or the Regents of the University of California. The views and opinions of authors expressed herein do not necessarily state or reflect those of the United States Government or any agency thereof or the Regents of the University of California.

A NEW MODEL FOR WELL TEST ANALYSIS IN A PURELY FRACTURED MEDIUM

Kenzi Karasaki, Jane C. S. Long, Paul A. Witherspoon

Earth Science Division
Lawrence Berkeley Laboratory
University of California
Berkeley, California 94720

Abstract

In a porous medium the flow conduits are small and a large number of conduits are connected to the well. For this reason the medium appears to behave like a continuum on the scale of the well test, and volumetric averaging and continuum approximations are justified. On the contrary, in a fractured medium, only a small number of fractures may intersect the pumping well. These particular fractures will be stressed by a large gradient under well test conditions. Consequently, the early time behavior will be dominated by these fractures. The volumetrically averaged permeability does not control flow in the vicinity of an active well. The individual fractures close to the well must be characterized in order to understand the well test behavior especially if the hydraulic parameters of these fractures are significantly different from the average values for the entire system.

In the present study, a new analytical model is proposed for well test problems in fracture networks where the matrix is impermeable. The model accounts for the difference in the flow regime around the active well from that of the system as a whole. The analytical solutions are presented in a series of type curves for ranges of dimensionless parameters. The flow propreties of the fracture system can be determined by curve matching.

Introduction

In the region near the pumping well, a single continuum approximation is not appropriate for modelling well tests[1]. This is because the inner boundary condition of a well test causes flow to converge on the few fractures which intersect the well. These fractures are macroscopic features compared to the well bore radius. However large the scale of observation may be, the characteristic length of the system still has to be the wellbore radius of the pumping well. In a porous medium the size of each flow conduit is microscopic and there are a large number of conduits connected to the well. In this case volumetric averaging and continuum approximations are justified. On the contrary, in a purely fractured medium, the small number of fractures that intersect the pumping well will be stressed by a large gradient. The volumetrically averaged permeability does not control flow in the vicinity of an active well. The individual fractures close to the well must be characterized in order to understand the well test behavior especially if the hydraulic parameters of these fractures are significantly different from the average values for the entire system.

In this study a new analytical solution is proposed for well test problems in purely fractured media based on a composite model with two concentric regions. The inner region contains a finite number of descrete fractures. The outer region is a classical porous medium. Similar composite models have been examined in the petroleum literature[2,3,4] but none include the effects of intra-fracture flow. The analysis of a well intersecting a single vertical fracture in a porous matrix has also been developed. However, in this case flow enters the fracture from the faces. In our model the fluid enters and exits the fractures only from their intersections with other fractures. A solution is obtained for a finite radius well. The solution is presented in a series of type curves, so that the flow propreties of the fracture system can be determined by curve matching.

Model Description

An iso-thermal well test problem in a homogeneously fractured formation of uniform thickness H is considered. The fractures are assumed to be vertical and extend from the top to the bottom of the formation. It is further assumed that the rock matrix is impermeable and all the hydraulic parameters are independent of pressure. No wellbore storage or damage is considered. The conceptual model of the well test in this system consists of two zones. In the outer region the usual equivalent porous medium approximation is assumed to hold, i.e., the flow properties of the fractures are volumetrically averaged and a single contiuum replaces the fractures. The hydraulic conductivity and the storage coefficient for the region are k_2 and S_{s_2}, respectively. The well is located in the center of the inner region and communicates with the outer region through a finite number (n) of fractures in the inner region. The radius of the well is r_w and the radius of the boundary between the inner and outer regions is r_f. All the fractures in the inner region have the same hydraulic aperture b and the hydraulic parameters k_1 and S_{s_1}. It is assumed that there is an infinitesimally thin ring of infinite conductivity between the two regions so that the otherwise incompatible boundaries can be matched. Figure-1 illustrates the model. The details of the solution are given below and the final result can be found in Equation (28). We then examine the assymptotic behavior in small and large time in order to provide simpler solutions and check the results.

The governing equation for the inner region is that for one dimensional unsteady-flow,

$$\frac{\partial^2 h_1}{\partial r^2} = \frac{1}{\alpha_1} \cdot \frac{\partial h_1}{\partial t} . \tag{1a}$$

where the hydraulic diffusivity, $\alpha = k/S_s$. For the outer region the usual radial flow equation describes the flow.

$$\frac{\partial^2 h_2}{\partial r^2} + \frac{1}{r} \cdot \frac{\partial h_2}{\partial r} = \frac{1}{\alpha_2} \cdot \frac{\partial h_2}{\partial t} . \tag{1b}$$

The initial conditions and the boundary conditions for constant rate injection test are

$$h_1(r, 0) = 0 \quad (r_w \le r \le r_f) \tag{2}$$

$$h_2(r, 0) = 0 \quad (r_f \le r \le \infty) \tag{3}$$

$$-nk_1 bH \frac{\partial h_1}{\partial r} = Q \quad (r = r_w) . \tag{4}$$

For the continuity at the boundary of the inner and outer region, we have

$$h_1 = h_2 \quad (r = r_f) \tag{5}$$

$$nk_1 b \frac{\partial h_1}{\partial r} = 2\pi r k_2 \frac{\partial h_2}{\partial r} \quad (r = r_f) . \tag{6}$$

The following dimensionless parameters are defined:

$$h_D = \frac{2\pi k_2 Hh}{Q} , \quad t_D = \frac{\alpha_2 t}{r_w^2} \cdot \frac{r_w^2}{r_f^2} = \frac{\alpha_2 t}{r_f^2} , \quad r_D = \frac{r}{r_f} ,$$

$$r_c = \frac{r_w}{r_f} , \quad \alpha_c = \frac{\alpha_1}{\alpha_2} , \quad \beta = \frac{nbk_1}{2\pi r_f k_2} . \tag{7}$$

Substituting into Eqs.(1a) and (1b) we obtain

$$\frac{\partial^2 h_{D_1}}{\partial r_D^2} = \frac{1}{\alpha_c} \frac{\partial h_{D_1}}{\partial t_D} \tag{8}$$

$$\frac{\partial^2 h_{D_2}}{\partial r_D^2} + \frac{1}{r_D} \frac{\partial h_{D_2}}{\partial r_D} = \frac{\partial h_{D_2}}{\partial t_D} . \tag{9}$$

In terms of the dimensionless parameters the initial and boundary conditions become

$$h_{D_1}(r_D, 0) = 0 \quad (r_c \le r_D \le 1) \tag{10}$$

$$h_{D_2}(r_D, 0) = 0 \quad (1 \le r_D \le \infty) \tag{11}$$

$$\frac{\partial h_{D_1}}{\partial r_D} = -\frac{1}{\beta} \quad (r_D = r_c) \tag{12}$$

$$h_{D_1} = h_{D_2} \quad (r_D = 1) \tag{13}$$

$$\frac{\partial h_{D_1}}{\partial r_D} = \frac{1}{\beta} \cdot \frac{\partial h_{D_2}}{\partial r_D} \quad (r_D = 1) \tag{14}$$

Solution Scheme

Laplace transforms can be used successfully to solve the equations simultaneously. The subsidiary equations are:

$$\frac{d^2 \bar{h}_{D_1}}{dr_D^2} = \frac{p}{\alpha_c} \bar{h}_{D_1} \tag{15}$$

$$\frac{d^2 \bar{h}_{D_2}}{dr_D^2} + \frac{1}{r_D} \cdot \frac{d\bar{h}_{D_2}}{dr_D} = p\bar{h}_{D_2} . \tag{16}$$

The transformed boundary conditions are

$$\frac{d\bar{h}_{D_1}}{dr_D} = -\frac{1}{\beta p} \quad (r_D = r_c) \tag{17}$$

$$\bar{h}_{D_1} = \bar{h}_{D_2} \quad (r_D = 1) \tag{18}$$

$$\frac{d\bar{h}_{D_1}}{dr_D} = \frac{1}{\beta} \frac{d\bar{h}_{D_2}}{dr_D} \quad (r_D = 1) . \tag{19}$$

The general solutions for Eqs.(15) and (16) are of the form:

$$\bar{h}_{D_1} = A \cosh(\sqrt{p/\alpha_c} \cdot r_D) + B \sinh(\sqrt{p/\alpha_c} \cdot r_D) \tag{20}$$

$$\bar{h}_{D_2} = C\, I_0(\sqrt{p} \cdot r_D) + D\, K_0(\sqrt{p} \cdot r_D) \tag{21}$$

where I_0 and K_0 are modified bessel functions of zeroth order of the first and second kind, respectively. The coefficient C in Eq.(21) is found to be nil since we expect the solution to be bounded for $r_D \to \infty$. Eqs.(20) and (21) are substituted into Eqs.(17), (18) and (19), and the following set of equations are obtained.

$$A\sqrt{p/\alpha_c} \sinh(\sqrt{p/\alpha_c} \cdot r_c) + B\sqrt{p/\alpha_c} \cosh(\sqrt{p/\alpha_c} \cdot r_c) = -\frac{1}{\beta p}$$

$$A \cosh\sqrt{p/\alpha_c} + B \sinh\sqrt{p/\alpha_c} = DK_0(\sqrt{p}) \tag{22}$$

$$A\sqrt{p/\alpha_c} \sinh\sqrt{p/\alpha_c} + B\sqrt{p/\alpha_c} \cosh\sqrt{p/\alpha_c} = -\frac{D}{\beta}\sqrt{p}\, K_1(\sqrt{p})$$

Eqs.(22) are solved for A,B and D.

$$A = \frac{\sqrt{\alpha_c}}{\beta p \sqrt{p}\, \Delta} \times \left[\sqrt{\alpha_c} K_1(\sqrt{p}) \sinh\sqrt{p/\alpha_c} + \beta K_0(\sqrt{p}) \cosh\sqrt{p/\alpha_c}\right]$$

$$B = -\frac{\sqrt{\alpha_c}}{\beta p \sqrt{p}\, \Delta} \times \left[\sqrt{\alpha_c} K_1(\sqrt{p}) \cosh\sqrt{p/\alpha_c} + \beta K_0(\sqrt{p}) \sinh\sqrt{p/\alpha_c}\right] \tag{23}$$

$$D = \frac{\sqrt{\alpha_c}}{p\sqrt{p}\, \Delta}$$

where

$$\Delta = \sqrt{\alpha_c} K_1(\sqrt{p}) \cosh\left[\sqrt{p/\alpha_c} \cdot (1-r_c)\right] + \beta K_0(\sqrt{p}) \sinh\left[\sqrt{p/\alpha_c} \cdot (1-r_c)\right]$$

Substituting A,B and D back into Eqs.(20) and (21), the solutions in the Laplace domain are obtained:

$$\bar{h}_{D_1} = \frac{\sqrt{\alpha_c}}{\beta p \sqrt{p}\, \Delta} \left\{\sqrt{\alpha_c} K_1(\sqrt{p}) \sinh\left[\sqrt{p/\alpha_c} \cdot (1-r_D)\right] + \beta K_0(\sqrt{p}) \cosh\left[\sqrt{p/\alpha_c} \cdot (1-r_D)\right]\right\} \tag{24}$$

$$\bar{h}_{D_2} = \frac{\sqrt{\alpha_c}}{p\sqrt{p}\, \Delta} K_0(\sqrt{p} \cdot r_D) \tag{25}$$

Inversion of $\bar{h}_{D_1}$

The inversion theorem is applied to $p\bar{h}_{D_1}$[5].

$$L^{-1}\{p\bar{h}_{D_1}\} = \frac{1}{2\pi i} \int_{\gamma - i\infty}^{\gamma + i\infty} p\bar{h}_{D_1} e^{pt_D} dp$$

$$= \frac{1}{2\pi i} \int_{\gamma - i\infty}^{\gamma + i\infty} \frac{\sqrt{\alpha_c}\, e^{pt_D}}{\beta\sqrt{p}\, \Delta} \left\{\sqrt{\alpha_c} K_1(\sqrt{p}) \sinh\left[\sqrt{p/\alpha_c} \cdot (1-r_D)\right] + \beta K_0(\sqrt{p}) \cosh\left[\sqrt{p/\alpha_c} \cdot (1-r_D)\right]\right\} dp \tag{26}$$

The integrand has a branch point at $p=0$. We consider the contour Γ in Figure-2. Since there are no singularities within Γ,

$$\oint_{\Gamma} = \int_A^B + \int_B^C + \int_C^D + \int_D^E + \int_E^F + \int_F^A = 0 ,$$

so that

$$\int_A^B = - \left[\int_B^C + \int_C^D + \int_D^E + \int_E^F + \int_F^A \right] .$$

Therefore,

$$L^{-1}\{p\bar{h}_{D_1}\} = \lim_{\substack{R\to\infty \\ \epsilon\to 0}} \frac{1}{2\pi i}\int_A^B$$

$$= - \frac{1}{2\pi i}\lim_{\substack{R\to\infty \\ \epsilon\to 0}} \left[\int_B^C + \int_C^D + \int_D^E + \int_E^F + \int_F^A \right] ,$$

where R is the radius of the outer circle and ϵ the radius of the inner. It can be shown that

$$\lim_{R\to\infty}\int_B^C = \lim_{R\to\infty}\int_F^A = 0 .$$

Also, by letting $p=\epsilon e^{i\theta}$ and taking the limit as $\epsilon\to 0$,

$$\lim_{\epsilon\to 0}\int_D^E = 0 .$$

On CD, let $p=\mu^2 e^{i\pi}$ and on EF let $p=\mu^2 e^{-i\pi}$ and using the identity:

$$K_\nu(ze^{\pm\frac{1}{2}\pi i}) = \pm\frac{1}{2}\pi i e^{\pm\frac{1}{2}\nu\pi i}\left[-J_\nu(z)\pm iY_\nu(z)\right] ,$$

we obtain

$$\frac{1}{2\pi i}\lim_{\substack{R\to\infty \\ \epsilon\to 0}}\int_C^D = \frac{\sqrt{\alpha_c}}{\beta\pi i}\int_0^\infty e^{-\mu^2 t_D}\frac{\Lambda+i\Omega}{\Psi+i\Theta}d\mu$$

$$\frac{1}{2\pi i}\lim_{\substack{R\to\infty \\ \epsilon\to 0}}\int_E^F = \frac{\sqrt{\alpha_c}}{\beta\pi i}\int_0^\infty e^{-\mu^2 t_D}\frac{-\Lambda+i\Omega}{-\Psi+i\Theta}d\mu$$

, where

$$\Lambda = -\sqrt{\alpha_c}\,J_1(\mu)\sin\left(\frac{1-r_D}{\sqrt{\alpha_c}}\mu\right) - \beta J_0(\mu)\cos\left(\frac{1-r_D}{\sqrt{\alpha_c}}\mu\right) \tag{27a}$$

$$\Omega = \sqrt{\alpha_c}\,Y_1(\mu)\sin\left(\frac{1-r_D}{\sqrt{\alpha_c}}\mu\right) + \beta Y_0(\mu)\cos\left(\frac{1-r_D}{\sqrt{\alpha_c}}\mu\right) \tag{27b}$$

$$\Psi = -\sqrt{\alpha_c}\,J_1(\mu)\cos\left(\frac{1-r_c}{\sqrt{\alpha_c}}\mu\right) + \beta J_0(\mu)\sin\left(\frac{1-r_c}{\sqrt{\alpha_c}}\mu\right) \tag{27c}$$

$$\Theta = \sqrt{\alpha_c}\,Y_1(\mu)\cos\left(\frac{1-r_c}{\sqrt{\alpha_c}}\mu\right) - \beta Y_0(\mu)\sin\left(\frac{1-r_c}{\sqrt{\alpha_c}}\mu\right) \tag{27d}$$

Therefore

$$L^{-1}\{p\bar{h}_{D_1}\} = -\frac{1}{2\pi i}\lim_{\substack{R\to\infty \\ \epsilon\to 0}}\left[\int_C^D + \int_E^F\right]$$

$$= \frac{2\sqrt{\alpha_c}}{\pi\beta}\int_0^\infty e^{-\mu^2 t_D}\frac{\Lambda\cdot\Theta - \Omega\cdot\Psi}{\Psi^2+\Theta^2}d\mu .$$

Simplifying and using the recurrence formula:

$$J_\nu(z)Y_\nu'(z) - Y_\nu(z)J_\nu'(z) = \frac{2}{\pi z} ,$$

$$L^{-1}\{p\bar{h}_{D_1}\} = \frac{4\alpha_c}{\pi^2}\int_0^\infty \frac{e^{-\mu^2 t_D}}{\mu}\cdot\frac{\cos\left(\frac{r_D-r_c}{\sqrt{\alpha_c}}\mu\right)}{\Psi^2+\Theta^2}d\mu$$

Finally, by the convolution theorem we obtain

$$h_{D_1} = \frac{4\alpha_c}{\pi^2}\int_0^{t_D}\int_0^\infty \frac{e^{-\mu^2\tau}}{\mu}\cdot\frac{\cos\left(\frac{r_D-r_c}{\sqrt{\alpha_c}}\mu\right)}{\Psi^2+\Theta^2}d\mu d\tau$$

$$= \frac{4\alpha_c}{\pi^2}\int_0^\infty \frac{1-e^{-\mu^2 t_D}}{\mu^3}\cdot\frac{\cos\left(\frac{r_D-r_c}{\sqrt{\alpha_c}}\mu\right)}{\Psi^2+\Theta^2}d\mu$$

$$(r_c \le r_D \le 1) \tag{28}$$

Eq.(28) can be used to evaluate h_{D_1} at r_D as a function of t_D for given α_c, β and r_c. Figure-3 is a log-log plot of h_{D_1} vs. t_D at $r_D=r_c=0.01$ for ranges of α_c and β. All the curves have characteristic initial half-slope straight line portion, which is the evidence of linear flow. A curve matching technique can be used to analyze well test data with such characteristics. If a unique match of the data to one of the curves generated by Eq.(28) can be found, α_c, β and r_c can be determined. The pressure and time match yield two more equations which give k_2 and the product $S_{s_2}r_f^2$. If k_1 can be expressed in terms of b using the parallel plate analogy, i.e., $k = b^2\rho g/12\mu$ where ρ, g and μ are fluid density, gravity constant and fluid viscosity, respectively, and if n, the number of fracture intersecting the well, is known, then the unknowns k_1, S_{s_1}, k_2, S_{s_2}, and r_f can all be calculated from Eqs.(7).

In Figure-4, h_{D_1} is evaluated using Eq.(28) for various values of r_c with $\alpha_c=2.0$ and $\beta=0.7$. Note that when $r_c = 1.0$, i.e., zero inner zone thickness, the curve is identical to that of van Everdingen and Hurst[6]. As can be seen in Figure-4, h_{D_1} is not very sensitive to r_c for $r_c < 0.1$. Therefore, it may be very difficult to determine r_c directly from the match for $r_c = r_w/r_f < 0.1$. This would leave only four equations to work with. In such a case, either one of S_{s_1}, k_1, S_{s_2}, or r_f must be estimated a priori in order to determine the rest. An observation well is needed to determine S_{s_2} a priori; k_1 and r_f will probably never be known a priori. One might assume S_{s_1} to be equal to fluid compressibility as a possible first trial.

Large Time Solution for Region 1

For small values of z,

$$K_0(z) \approx -\ln\frac{Ez}{2} - \frac{z^2}{4}\cdot\left(\ln\frac{Ez}{2} - 1\right) + \cdots \tag{29a}$$

$$K_1(z) \approx \frac{1}{z} + \frac{z}{2}\cdot\left(\ln\frac{Ez}{2} - \frac{1}{2}\right) + \cdots \tag{29b}$$

$$\cosh z \approx 1 + \frac{z^2}{2} + \cdots \tag{29c}$$

$$\sinh z \approx z + \frac{z^3}{6} + \cdots \tag{29d}$$

where $\ln E = \gamma = 0.577215665$ (Euler's constant). Substituing Eq.(29) into (24) and rearranging,

$$\bar{h}_{D_1} \approx \frac{1}{p}\left\{ \frac{1-r_D}{\beta} - \ln\frac{E\sqrt{p}}{2} + \right.$$

$$\left. + \left[\frac{1-r_D}{\beta} - \frac{1}{2} - \frac{(1-r_D)^2}{\alpha_c} \right] \cdot \frac{p}{2} \cdot \ln\frac{E\sqrt{p}}{2} + \cdots \right\} \times$$

$$\times \left\{ 1 + p \cdot \left[\frac{1}{2} - \frac{\beta(1-r_c)}{\alpha_c} \right] \cdot \ln\frac{E\sqrt{p}}{2} + \cdots \right\}^{-1}$$

$$\approx \frac{1}{p} \cdot \left\{ \frac{1-r_D}{\beta} - \ln\frac{E\sqrt{p}}{2} + \right.$$

$$\left. + p \cdot \left[\frac{1}{2} - \frac{\beta(1-r_c)}{\alpha_c} \right] \cdot (\ln\frac{E\sqrt{p}}{2})^2 + \cdots \right\}$$

so that

$$h_{D_1} = L^{-1}\{\bar{h}_{D_1}\}$$

$$\approx \frac{1-r_D}{\beta} + \frac{1}{2} \cdot \left\{ 1 + \frac{1}{t_D} \cdot [\frac{1}{2} - \frac{\beta(1-r_c)}{\alpha_c}] \right\} \times$$

$$\times (-\gamma + \ln 4t_D) + \cdots$$

$$\approx \frac{1-r_D}{\beta} + \frac{1}{2} \cdot (-\gamma + \ln 4t_D) \tag{30}$$

Eq.(30) shows that for large t_D, h_{D_1} can be approximated by a logarithmic function of t_D. The lower limit of t_D for which this approximation is valid is a function of β, α, and r_c as can be seen in the derivation of Eq.(30). On a semi-log graph, Eq.(30) is would be a straight line identical to the solution for a homogeneous porous medium except for the constant $(1-r_D)/\beta$. This, in effect, can be thought as apparent "skin". Therefore, k_2 can be obtained in the usual manner but the calculation of the storage coefficient in the conventional manner may result in incorrect value of that parameter by a factor given by

$$\frac{S_{s_2}^{\,*}}{S_{s_2}} = \frac{r_f^2}{r_w^2} \exp\left[-\frac{2(1-r_w/r_f)}{\beta} \right]. \tag{31}$$

Small Time Solution for Region 1

Remembering for small z,

$$K_\nu(z) = \left(\frac{\pi}{2z}\right)^{1/2} \cdot e^{-z} \cdot \left\{ 1 + \frac{4\nu^2 - 1}{8z} + O(\frac{1}{z^2}) \right\}$$

Since $r_c < 1$,

$$\bar{h}_{D_1} \approx \frac{\sqrt{\alpha_c} \cdot e^{-\sqrt{p/\alpha_c}(r_D - r_c)}}{\beta p \sqrt{p}} \times$$

$$\times \left[1 - \frac{\sqrt{\alpha_c} - \beta}{\sqrt{\alpha_c} + \beta} \left(e^{-2\sqrt{p/\alpha_c}(1-r_D)} + e^{-2\sqrt{p/\alpha_c}(1-r_c)} \right) + \cdots \right]$$

Then at the pumping well, $r_D = r_c$,

$$h_{D_1} = L^{-1}\{\bar{h}_{D_1}\}$$

$$\approx \frac{2\sqrt{\alpha_c}}{\sqrt{\pi}\beta} \cdot \sqrt{t_D} \cdot \left[1 - 2 \cdot \frac{\sqrt{\alpha_c} - \beta}{\sqrt{\alpha_c} + \beta} \cdot e^{-(1-r_c)^2/\alpha_c t_D} \right] +$$

$$+ \frac{4}{\beta} \frac{\sqrt{\alpha_c} - \beta}{\sqrt{\alpha_c} + \beta} \cdot (1 - r_c) \cdot erfc \frac{1 - r_c}{\sqrt{\alpha_c t_D}} + \cdots \tag{32}$$

From Eq.(32), it is assured that for small t_D, h_{D_1} exhibits half slope straight line. Using the identities in Eqs.(7),

$$h_{t=1sec} = \frac{2Q}{nb\sqrt{\pi k_1 S_{s_1}}} \tag{33}$$

where $h_{t=1sec}$ is the value of h at $t = 1$sec obtained by extrapolating the straight line on log-log graph. Eq.(33) can be used to find bk_1 when n and S_{s_1} are known. If S_{s_2} is also known, Eq.(31) can then be used to find r_f without tedious curve matching.

Inversion of $\bar{h}_{D_2}$

It now remains to invert $\bar{h}_{D_2}$ to real space:

$$L^{-1}\{p\bar{h}_{D_2}\} = -\frac{2\sqrt{\alpha_c}}{\pi\beta} \int_0^\infty e^{-\mu^2 t_D} \frac{\Theta \cdot J_0(\mu r_D) + \Psi \cdot Y_0(\mu r_D)}{\Psi^2 + \Theta^2} d\mu .$$

So that

$$h_{D_2} = -\frac{2\sqrt{\alpha_c}}{\pi} \int_0^\infty \frac{1 - e^{-\mu^2 t_D}}{\mu^2} \cdot \frac{\Theta \cdot J_0(\mu r_D) + \Psi \cdot Y_0(\mu r_D)}{\Psi^2 + \Theta^2} d\mu$$

$$(r_D \geq 1) . \tag{34}$$

where Ψ and Θ are given by Eq.(27c) and (27d), respectively.

Large Time Solution for Region 2

Substituting Eqs.(29) into Eq.(25),

$$\bar{h}_{D_2} \approx \frac{1}{p}\left\{ -\ln\frac{E\sqrt{p}\,r_D}{2} + \right.$$

$$\left. + p\left[\frac{1}{2} - \frac{\beta(1-r_c)}{\alpha_c} \right] \cdot \ln\frac{E\sqrt{p}\,r_D}{2} \cdot \ln\frac{E\sqrt{p}}{2} + \cdots \right\}$$

Then,

$$h_{D_2} \approx \frac{1}{2}\left\{ 1 + \left[\frac{1}{2} - \frac{\beta(1-r_c)}{\alpha_c} \right] \frac{r_D^2}{t_D} \right\} (-\gamma + \ln\frac{4t_D}{r_D^2}) + \cdots$$

$$\approx \frac{1}{2}(-\gamma + \ln\frac{4t_D}{r_D^2}) \tag{35}$$

Small Time Solution for Region 2

For large p, noting that $r_c < 1$, Eq.(32) becomes

$$\bar{h}_{D_2} \approx \frac{2\sqrt{\alpha_c}}{\sqrt{\alpha_c} + \beta} \cdot \frac{e^{-\sqrt{p/\alpha_c}(1-r_c)}}{p\sqrt{p}} + \cdots ,$$

and now inverting $\bar{h}_{D_2}$, we have:

$$h_{D_2} \approx \frac{2\sqrt{\alpha_c}}{\sqrt{\alpha_c} + \beta} \times$$

$$\times \left[2\left(\frac{t_D}{\pi}\right)^{1/2} e^{-(1-r_c)^2/\alpha_c t_D} - \frac{1-r_c}{\sqrt{\alpha_c}} erfc \frac{1-r_c}{2\sqrt{\alpha_c t_D}} + \cdots \right] \tag{36}$$

This completes the large and small time solutions.

Example Application and Conclusion

Figure-5 illustrates an example of the procedure applied to find k_1, k_2, S_{s_2}, and r_f from a numerical well test simulation in the fracture network also shown in the figure. The numerical procedure employed here is discussed in Long[7] and Kanehiro[8]. A fit was found assuming S_{s_1} was known. The flow parameters for both regions calculated from the match point and from the equations for α_c and β were found to be very close to the input values. The calculated r_f was $4.9m$ in this case. In the actual network, the distance to the nearest intersection was $7.3m$ in one direction and $3.8m$ in the other, averaging $5.5m$.

If a fit can be found this analytical model can successfully be used to accurately determine the average storage coefficient of a fracture system from one-well test as well as the distance to the nearest fracture intersection, which in turn give us a clue to fracture spacing. Because there are an infinite number of curves for various combinations of α_c, β and r_c, an automatic curve fitting procedure by a computer is being investigated.

REFERENCES

1 Karasaki, K., Long, J.C.S., and Witherspoon, P.A.: "Well Test Analysis in Fracture Networks," Lawrence Berkeley Laboratory Annual Report in preparation, 1985.

2 Larkin, Bert K.: "Solutions to the Diffusion Equation for a Region Bounded by a Circular Discontinuity," *Soc. Pet Eng. J.* (June 1963) 113-115.

3 Ramey, H. J.: "Approximate Solutions for Unsteady Liquid Flow in Composite Reservoirs," *Journal of Canadian Petroleum Tech.* (March 1970), 32-37.

4 Cinco-L., Heber, Samiengo-V., F., and Dominguez-A., N.: "Transient Pressure Behavior for a Well with a Finite Conductivity Vertical Fracture," paper SPE 6014 presented at the SPE-AIME 51st Annual Fall Technical Conference and Exhibition, New Orleans, Oct. 3-6, 1976.

5 Carslaw, H.S. and Jaeger, J.C.: *Conduction of Heat in Solids*, Oxford: Clarendon Press, 1946.

6 van Everdingen, A.F. and Hurst, W.: "The Application of the Laplace Transformation to Flow Problems in Reservers," *Trans.*, AIME (1949) 186, 305-324.

7 Long, J.C.S., Remer, J.S., Wilson, C.R., and Witherspoon, P.A.: "Porous media equivalents for network of discontinuous fractures," *Water Resour. Res.*, 18(3), 645-658, 1982.

8 Kanehiro, B.Y., Wilson, C.R., and Karasaki, K.: "Transient analysis of groundwater flow in fracture networks," Lawrence Berkeley Laboratory Report LBL-15500, 1983.

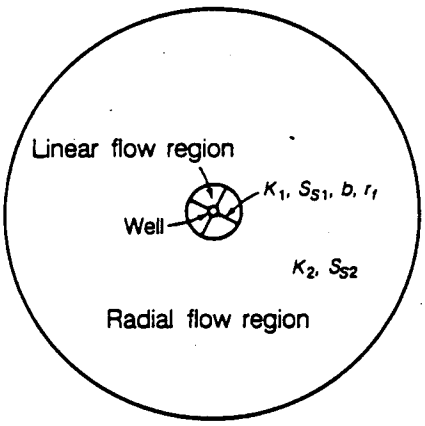

Figure-1 A schematic of the analytical model.

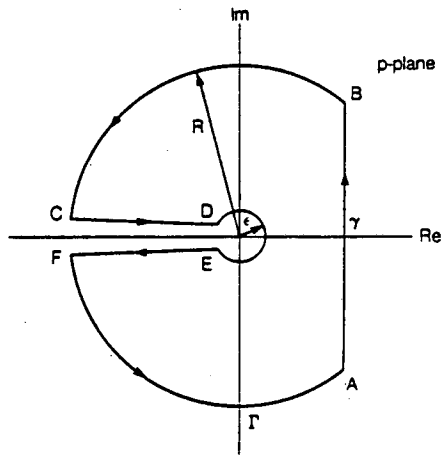

Figure-2 The contour path taken for Laplace inversion.

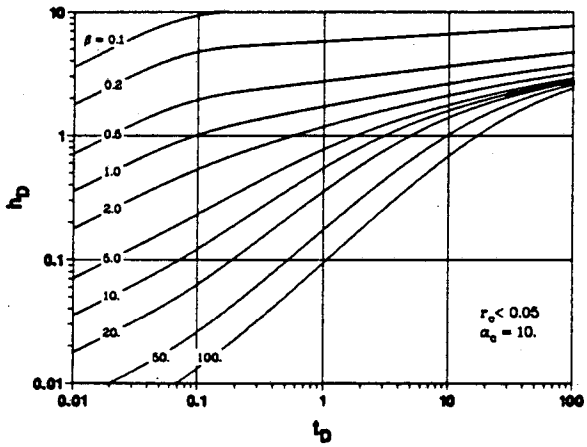

Figure-3a Dimensionless pressure for r_c<0.05 and α_c=10.

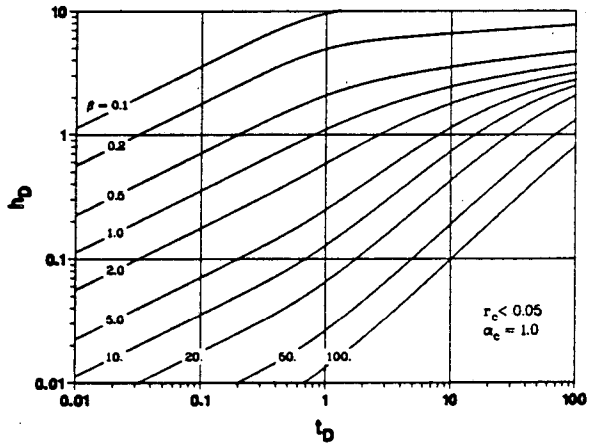

Figure-3b Dimensionless pressure for r_c<0.05 and α_c=1.0.

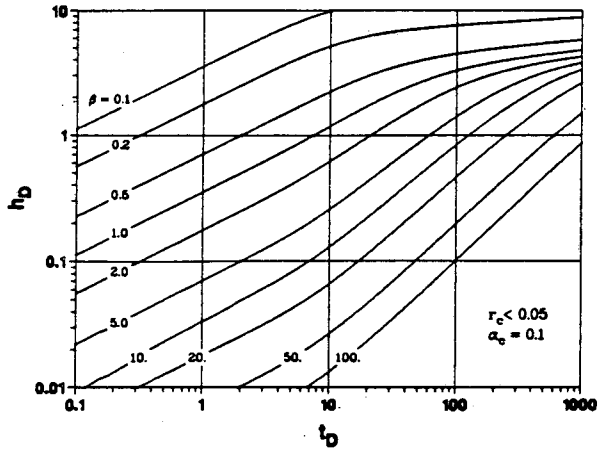

Figure-3c Dimensionless pressure for r_c<0.05 and α_c=0.1.

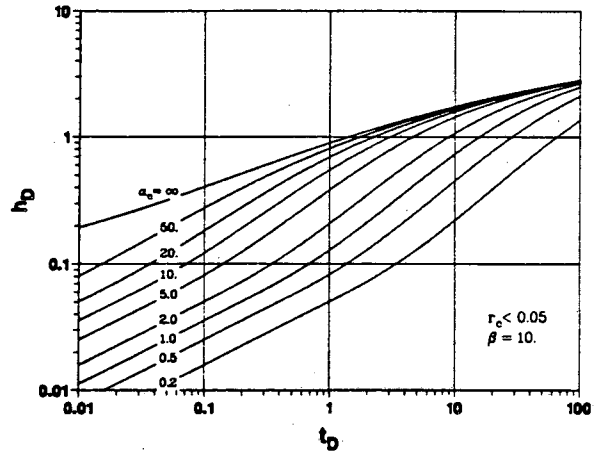

Figure-3d Dimensionless pressure for r_c<0.05 and β=10.

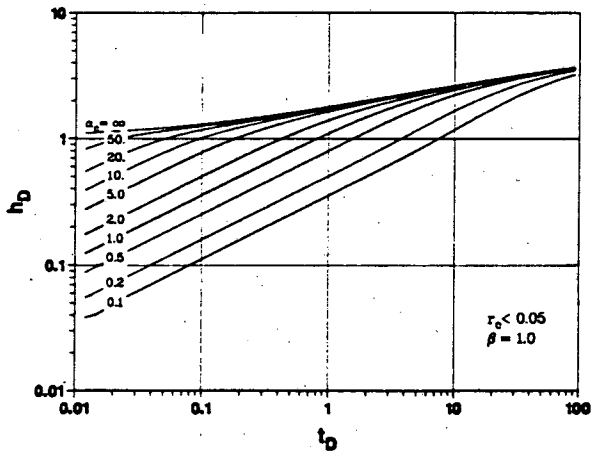

Figure-3e Dimensionless pressure for r_c<0.05 and β=1.0.

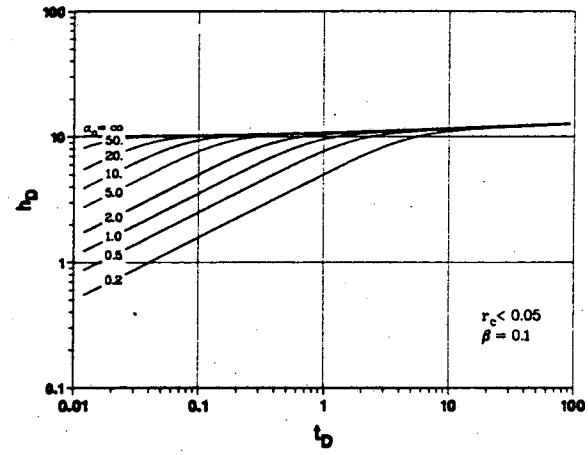

Figure-3f Dimensionless pressure for r_c<0.05 and β=0.1.

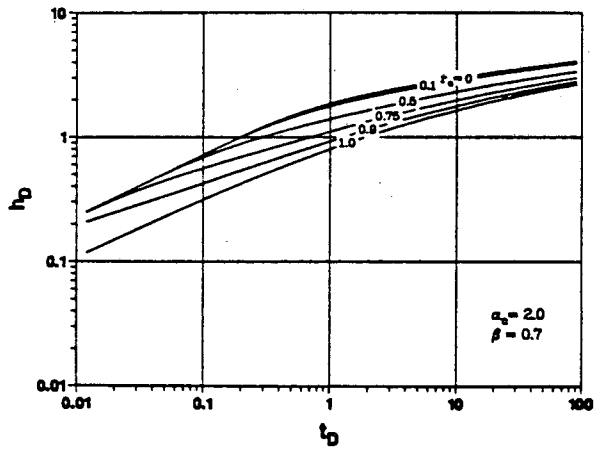

Figure-4 Dimensionless pressure for α_c=2.0 and β=0.7.

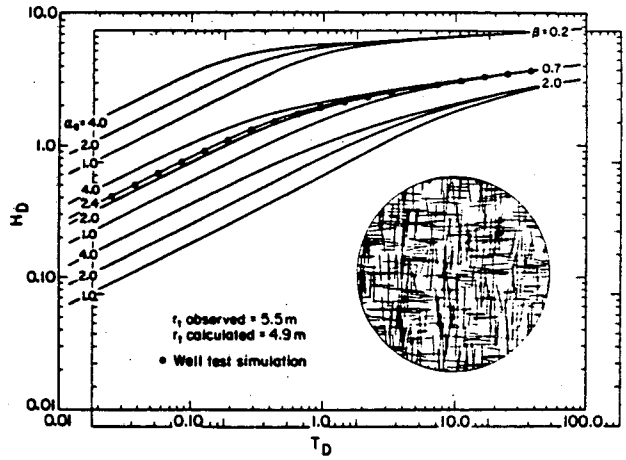

Figure-5 An example of curve matching technique applied to numerical well test simulation results.

This report was done with support from the Department of Energy. Any conclusions or opinions expressed in this report represent solely those of the author(s) and not necessarily those of The Regents of the University of California, the Lawrence Berkeley Laboratory or the Department of Energy.

Reference to a company or product name does not imply approval or recommendation of the product by the University of California or the U.S. Department of Energy to the exclusion of others that may be suitable.

TECHNICAL INFORMATION DEPARTMENT
LAWRENCE BERKELEY LABORATORY
UNIVERSITY OF CALIFORNIA
BERKELEY, CALIFORNIA 94720